Full length article

Hematopoietic tissue of *Macrobrachium rosenbergii* plays dual roles as a source of hemocyte hematopoiesis and as a defensive mechanism against *Macrobrachium rosenbergii* nodavirus infection

Pitchanee Jariyapong[a,b], Arnon Pudgerd[c,d], Nifareesa Cheloh[e], Ikuo Hirono[f], Hidehiro Kondo[f], Rapeepun Vanichviriyakit[d,g], Wattana Weerachatyanukul[g], Charoonroj Chotwiwatthanakun[d,h,*]

[a] *School of Medicine, Walailak University, Thasala District, Nakhonsrithammarat, 80161, Thailand*
[b] *Research Center of Excellence on Shrimp, Walailak University, Thasala District, Nakhonsrithammarat, 80161, Thailand*
[c] *Division of Anatomy, School of Medical Science, University of Phayao, Muang, Phayao, 56000, Thailand*
[d] *Center of Excellence for Shrimp Molecular Biology and Biotechnology (Centex Shrimp), Faculty of Science, Mahidol University, Rama VI Road, Bangkok, 10400, Thailand*
[e] *Faculty of Agriculture, Princess of Naradhiwas University, Mueang Narathiwat District, Narathiwat, 96000, Thailand*
[f] *Laboratory of Genome Science, Graduate School of Marine Science and Technology, Tokyo University of Marine Science and Technology, Konan 4-5-7, Minato, Tokyo, 108-8477, Japan*
[g] *Department of Anatomy, Faculty of Science, Mahidol University, Rama VI Road, Bangkok, 10400, Thailand*
[h] *Nakhonsawan Campus, Mahidol University, Nakhonsawan, 60130, Thailand*

ARTICLE INFO

ABSTRACT

White tail disease caused by *Macrobrachium rosenbergii* nodavirus (MrNV) infection takes place only in nauplii, not adults, of *M. rosenbergii* prawn. Hemocyte homeostasis and immune-related functions derived from the hematopoietic tissue (Hpt) in adult prawn are presumed to play roles in resisting viral infection. To elucidate the role of the Hpt cell response to MrNV, a comparative transcriptome analysis was performed with MrNV-infected prawn at various time intervals. The results showed that there were 462 unigenes that were differentially expressed between mock and infected samples. BlastX sequence analysis revealed that two proteins, crustacean hematopoietic factor (CHF) and cell growth-regulating zinc finger protein (Lyar), are involved in hemocyte hematopoiesis and are up-regulated during MrNV infection. In fact, genes involved in cell growth regulation and immunity were highly expressed at 6 h and decreased within 24 h post-infection. Localization studies in the Hpt tissue revealed the presence of anti-lipopolysaccharide factor (ALF) and CHF mRNAs in Hpt cells. Considering these findings, we concluded that resistance to MrNV infection in adult prawn is due to an increase in humoral immune factors and the acceleration of hemocyte homeostasis by the dual roles of the Hpt organ in *M. rosenbergii*.

1. Introduction

Macrobrachium rosenbergii (Mr) or giant freshwater prawn is considered one of the most economically important crustaceans for Asian countries. The establishment of specific-pathogen-free nauplii frequently fails due to contamination with viruses during preparation of broodstocks. One of the most common diseases that causes mass mortality of nauplii is white tail disease caused by *Macrobrachium rosenbergii* nodavirus (MrNV) together with extra small virus [1,2]. This infectious disease presents as whitish muscle and causes a massive loss at the postlarvae (PL) stage but does not cause any symptoms in adult prawn. Experimental challenges of adult prawn with either MrNV or white spot syndrome virus (WSSV) showed disease resistance, suggesting a well-developed, highly efficient immunity against the viruses in the adult animals [3,4]. Three well-established parameters, proPO, O_2^- and clotting time, significantly increase in hemolymph during WSSV clearance in adult prawn, whereas the total hemocyte number and superoxide dismutase activity decrease [5,6]. This result suggests that WSSV resistance might correspond to humoral immunity rather than cellular response.

During infection or injury, there is a notable decrease in the circulating hemocyte population; therefore, the survival of prawn relies

partly on newly synthesized hemocytes released from hematopoietic tissue (Hpt) [7]. Hpt is a specialized tissue that contains self-renewing stem cells that generate hemocytes, a process called hematopoiesis, throughout an animal's life [8]. It is hypothesized that this organ might play dual roles as a source of hemocyte proliferation and a humoral defensive mechanism during microbe infections. Proteomic analysis of Hpt from WSSV-infected red claw crayfish demonstrated an increase in many proteins participating in metabolic processes, signal transduction and especially immune enhancement pathways during the experimental infection [9]. It is thus presumed that humoral immunity-related proteins detected in the hemolymph of infected crayfish might be synthesized by Hpt during infection.

In this study, we determined the differential gene expression in Hpt of adult prawn during an experimental MrNV infection by next-generation sequencing to identify the important genes responsible for disease resistance. These findings will provide insight into the molecular defensive mechanism of Hpt against MrNV infection, which would be helpful for disease management of this prawn aquaculture under many unavoidable stressful conditions.

2. Materials and methods

2.1. MrNV inoculums

The MrNV inoculums were prepared and purified according to our published protocol [10]. Briefly, Sf9 cells were transfected with synthesized RNA1 and RNA2 using Cellfectin II reagent (Invitrogen, Camarillo, CA) following the manufacturer's instructions. At 96 h, the transfected cells were then collected and homogenized in PBS. The supernatant was collected for stepwise centrifugation to purify viruses. The viral pellet was finally resuspended in PBS, and the viral copy numbers were quantitated by real-time PCR using specific primers for MrNV (Table 1). A standard curve for quantifying the MrNV viral genomic copy number was obtained from a 10-fold serial dilution of a pGEM T-easy vector containing the full length of synthesized RNA2 (1175 bp). The PCR thermal conditions consisted of 45 cycles of denaturation at 94 °C for 30 s, annealing at 53 °C for 30 s, and extension at 72 °C for 30 s. The stock was used at a concentration of 10 copy μL^{-1} for intramuscular (IM) injection into the prawn.

2.2. Animals and MrNV challenging

A total of 40 adult prawn with approximately 15 ± 0.8 g body weight were obtained from a commercial farm in Ratchaburi Province, Thailand. They were screened for contamination with 8 infectious viruses, including yellow head virus (YHV), gill-associated virus (GAV), white spot syndrome virus (WSSV), monodon baculovirus (MBV), infectious hypodermal hematopoietic necrosis virus (IHHNV), hepatopancreatic parvovirus (HPV), Taura syndrome virus (TSV) and Laem-Singh virus (LSNV), by PCR or RT-PCR, maintained in 300 L tanks,

Table 1
Primer used in this study.

Name	Primer sequence (5′–3′)	Purpose
RNA2	(F) 5′- AAAGGATATTCGATATTCTATCATC-3′	Virus copy number
	(R) 5′- ACGTCACTCCTAGCACTTCT-3′	
ALF	(F) 5′- GTCTTGGGTTGTTTTGGTAA-3′	RT-qPCR
	(R) 5′- CATCGTTACTTCCCACTTGT-3′	
HSP70	(F) 5′- GTCCTGATGAAGATGAAGGA-3′	RT-qPCR
	(R) 5′- CCTTGCCACTTGTTACTTTC -3′	
CHF	(F) 5′- GAGGGTCTGTCTTGCTACTG-3′	RT-qPCR
	(R) 5′- GGTACTTCTCCTCGTCTCCT-3′	
MSO	(F) 5′- TCGCAGTTGTGTATTTGTGT-3′	RT-qPCR
	(R) 5′- AAAATAATGCTCGAGTCCAA-3′	
EF-1α	(F) 5′- ATGTCATGGTGGAAGAAGAG -3′	RT-qPCR
	(R) 5′- AAAGTTGACCACCATACCAG -3′	

supplied with filtered water at 30 ± 0.5 °C, and fed daily with commercial food before use.

Groups of ten specific pathogen-free prawn were intramuscularly injected with 100 μL of 10 copy μL^{-1} MrNV inoculum, and their hematopoietic tissue was collected at 6 and 24 h post injection for next-generation sequencing (NGS) and *in situ* hybridization. Untreated prawn was employed as negative controls in the experiments.

2.3. Total RNA isolation, next-generation sequencing and bioinformatics

Total RNA was extracted from the Hpt of the mock and infected groups at the indicated time points using TriPure isolation reagent (Roche, Mannheim, Germany) according to the manufacturer's protocol. RNA from 5 individuals in each group was quantitated and pooled for NGS and qRT-PCR.

To construct each validated library, the pooled RNAs at different time points were processed following the TruSeq® RNA sample preparation protocol. Three validated libraries (10 nM of pooled RNA from experimental 6 h and 24 h groups and the control group) were pooled for validated library normalization and subjected to pair-end RNA sequencing using an Illumina next-generation sequencing MiSeq instrument (Illumina, San Diego, U. S. A.). The raw sequence reads were trimmed to remove adapter sequences, unclear nucleotides, low quality score and short read length sequences using the Trimmomatic program [11]. After the initial quality control step, the adapter-free reads were subjected to transcriptome assembly using the Trinity software [12]. The outputs of all the transcripts were saved in FASTA format. To obtain the relative expression level between the negative control and each experimental infection group, transcript counts were normalized to the total number of produced transcripts per sample. Statistical tests with a significance level of $P < 0.001$ and calculated fold changes were included to identify candidates for differential gene expression (DEG). All up- and down-regulated genes that met the $P < 0.001$ criterion were further subjected to gene ontology analysis against NCBI nonredundant protein (NR) and UniProt databases using the Blast2GO bioinformatics software version 4.0.

2.4. Sequence analysis

Searches for homologous nucleotide or protein sequences in sequence databases were carried out using the BLASTX program. Protein translations were created using the EXPASY web server (http://au.expasy.org/). Multiple protein domain sequence alignments and phylogeny interference were performed using ClustalW (Thompson et al., 1994) and a molecular evolutionary genetics analysis program (MEGA). A putative three-dimensional model was computed using SWISS-MODEL [13].

2.5. Real-time RT-PCR

The relative expression of genes involved in cell growth regulation and immunity with significant alterations was validated by real-time RT-PCR using the specific primers listed in Table 1. The first strand cDNA templates were produced using an iScript™ cDNA Synthesis Kit (Bio-Rad, Philadelphia, PA) according to the manufacturer's protocol. qRT-PCR was carried out with an Applied Biosystems 7300 real-time PCR system (Thermo Fisher Scientific Inc., Waltham, MA) with a master mix that contained $2 \times$ SsoFast EvaGreen Supermix (Bio-Rad, Philadelphia, PA) according to the manufacturer's protocol. The qRT-PCR protocol consisted of a holding step at 95 °C for 10 s, followed by 35 cycles of denaturation at 95 °C for 30 s, annealing at 55 °C for 30 s, elongation at 72 °C for 1 min, and final elongation at 72 °C for 5 min. A standard curve was generated from ten serial dilutions of the pooled cDNA from the samples. The correlation coefficients for the standard curves were > 0.995 for all genes. Relative expression levels were determined by the $2^{\Delta\Delta Ct}$ method using EF-1α as the internal control and

presented as a relative expression ratio. The value of each variable was expressed as the mean ± SE. Statistical analysis was performed using SPSS software (Ver 17.0), and the significance between groups at a significance level of $p < 0.05$ was determined by one-way ANOVA.

2.6. In situ hybridization

The Hpt of untreated and virally infected groups were fixed in Davidson's fixative prior to the tissue processing steps, which include dehydration, clearing and embedding. Tissues were cut at 4 μm thick and subjected to *in situ* hybridization (ISH) according to a previously described protocol [14]. The digoxigenin (DIG)- labeled DNA probe was synthesized by the incorporation of digoxigenin-11-dUTP (Roche, Germany) during PCR using specific primers (Table 1). Micrographs were obtained using a Nikon E600 light microscope.

3. Results

3.1. Transcriptome analysis of Hpt post MrNV infection

Total RNA samples from the Hpt cells of control and infected prawn were extracted, purified and subjected to cDNA library construction. Three cDNA libraries each with a labeled index were processed for RNA sequencing. After removing low-quality sequences, 6,486,352 *(6.5G)*, 4,498,411 *(4.5G)* and 6,325,636 *(6.3G)* clean reads were obtained from control *(SRX3289952)* and MrNV-infected samples at 6 h *(SRX3289951)* and 24 h *(SRX3289953)*, respectively, representing a total of 17,310,399 *(17.3G)* clean reads. By means of the Trinity program, the assembly of all reads in the three libraries generated 63,894 contigs with an average of 713 nucleotide lengths. To identify the DEGs involved in MrNV infection in the Hpt, the unigenes in infected samples were normalized and compared to those in the control sample using the edgeR program with a threshold absolute value of log 2-fold-change and FDR < 0.001. The results showed that 462 unigenes were differentially expressed between the infected and control groups. After injection with MrNV, 281 up-regulated genes and 181 down-regulated genes were observed at 6 h post infection (p. i.) (Fig. 1). The top 20 up- and down-regulated unigenes are listed (Tables 2 and 3). Numerous
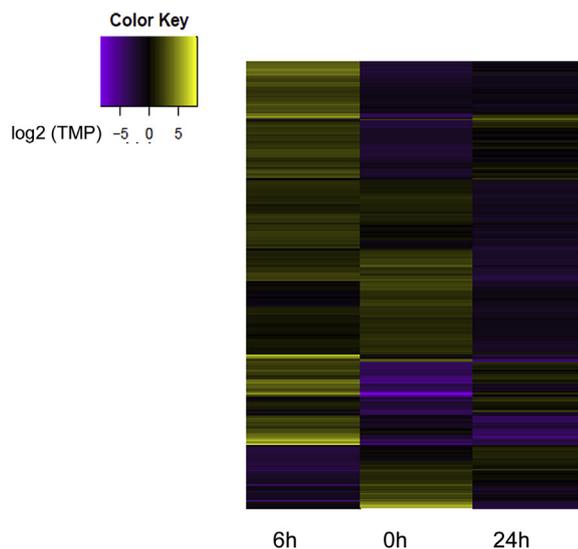

Fig. 1. RNA expression levels for 462 unigenes at 3 time points (0, 6, and 24 h p.i) in the Hpt cells of MrNV-challenged prawn. Gene activity during infection is shown in log 2-transformed transcripts per million (TPM). Each row represents a single gene, and each column represents the time of infection. Experimental sample genes in yellow and purple are up- and down-regulated, respectively. (For interpretation of the references to colour in this figure legend, the reader is referred to the Web version of this article.)

DEGs involved in various immune processes and cell growth regulation were found in the infected group compared with the control group (Table 4).

3.2. Functional annotation analysis of Hpt transcriptome sequences

All sequences from the 462 unigenes were aligned according to the NCBI NR, Kyoto Encyclopedia of Genes and Genome (KEGG) and Swiss-Prot databases using the Blast2GO program. Three GO categories comprising biological processes (BP), cellular components (CC) and molecular function (MF) were obtained. In the category of BP, most unigenes were involved in the cellular process, metabolic process, and single-organism process. In the CC category, the most represented were cell, cell part, and organelle. With respect to the MF category, binding, catalytic activity and structural molecular activity were the dominant groups. Species distribution aligned sequences revealed that unigenes matched sequences from seven top-hit species, i.e., *Hyalella Azteca*, *Macrobrachium rosenbergii*, *Penaeus monodon*, *Procambarus clarkia*, *Litopenaeus vannamei*, *Eriocheir sinensis*, *Scylla paramamosain*, *Crassostrea gigas* and *Zootermopsis nevadensis*, which belong to Arthropoda and Mollusca.

3.3. Characterization of MrCHF and MrLyar protein

According to the species distribution sequence analysis, 462 unigenes were matched to other species rather than Mr. It is inferred that Mr Hpt comprised several uncharacterized proteins with unknown function. BLASTX searching in the EST databases revealed that two Mr Hpt proteins shared 39% and 52% amino acid sequence identity with the crustacean hematopoietic factor-like protein (CHF) of *L. Vannamei* and the cell growth-regulating nucleolar protein (Lyar) of *A. Californica*, respectively. The characteristics of these proteins were verified as detailed below.

3.3.1. MrCHF protein

The *Mr*CHF ORF of 258 bp encoded a deduced protein of 121 amino acids *(Acc. No. MH595490)*. A putative conserved domain search revealed a similarity to insulin-like growth factor binding domain proteins *(IGFBP)* from various animals (Fig. 2A). The highest similarity match was with the protein sequence from the mouse, followed by decreasing homology with bird, frog and monkey IGFBP (Fig. 2B). A putative three-dimensional model shown in Fig. 2C was generated using the E69 deletion mutant single insulin-like growth factor binding domain protein *(SIBD-1)* from *Cupiennius salei* [15] as a template given its 37.84% identity.

3.3.2. MrLyar

The 1070 bp ORF of *Mr*Lyar encoding a deduced 323 amino acid protein *(Acc. No. MH626731)* contained conserved domain similarity to a cell growth-regulating zinc finger protein *(zf-Lyar)* that is involved in cell growth regulation in vertebrates and invertebrates *(Fig. 3A)*. The phylogenetic tree showed the close relationship of *Mr*Lyar from the highest to lowest with Lyar of mouse, roundworm, single-celled heterokont parasites and soil-living amoeba, respectively *(Fig. 3B)*. The putative three-dimensional model of *Mr*Lyar protein shown in Fig. 3C was generated from two published model templates [16,17].

3.4. Localization of MrCHF and MrALF genes in the hematopoietic tissue

Histological study revealed that Mr Hpt is arranged as lobules and encompasses at least 3 different cell types corresponding to the developmental stages of hemocytes. To determine whether Hpt cells express both genes related to cell growth and the immune system, we performed *in situ* hybridization of the *Mr*CHF and *Mr*ALF genes, which were highly expressed at 6 hpi. *Mr*CHF mRNA is highly expressed in the densely packed cells presumed to be the precursor cells located at the

Table 2
Top 20 up-regulated genes at 6 h post infection.

No	Protein/Gene description	Length	E-value	Fold change (log2)		Ontology (level 2)
				6 h	24 h	
1	Male reproductive-related serum amyloid A	226	8.03E-41	+ 5.0808	+ 1.0282	CC, BP
2	Protease inhibitor Epi 9	475	2.32E-08	+ 6.0974	− 2.6385	BP
3	Cytochrome c oxidase subunit mitochondrial-like	208	3.05E-13	+ 4.0513	0.1970	BP
4	Kazal-type serine protease	564	5.09E-06	+ 5.7540	− 2.7074	MF,CC, BP
5	DNA topoisomerase 2-alpha	281	6.53E-17	+ 4.0512	0.5654	N/A
6	F-box only 15	377	1.67E-22	+ 3.1594	+ 2.2483	N/A
7	Cuticle CP575-like	385	1.32E-19	+ 2.0530	+ 1.4763	N/A
8	Crustin 3	706	7.95E-53	+ 3.4545	+ 1.6154	MF,CC, BP
9	Anti-lipopolysaccharide factor 1	948	3.30E-60	+ 3.9257	+ 0.5031	N/A
10	Single VWC domain 1	323	6.97E-15	+ 4.2304	+ 0.0708	N/A
11	Cuticle pro	897	3.58E-54	+ 2.6060	+ 1.6304	MF
12	WW domain-containing -like	332	3.59E-06	+ 4.5107	− 1.9258	N/A
13	DNA topoisomerase 2-alpha	535	3.23E-13	+ 3.8245	− 0.3129	N/A
14	Proteasome subunit alpha type-4	295	2.60E-10	+ 3.9764	− 4.2158	MF,CC, BP
15	F-box only 15	750	6.31E-37	+ 3.1291	− 0.2450	N/A
16	Cuticle 1	275	1.42E-25	+ 1.5181	+ 1.8138	MF
17	Clip-domain serine protease	1341	4.41E-65	+ 3.7328	− 0.6595	MF, BP
18	Cuticular 34	445	2.22E-39	+ 1.2456	+ 1.4273	MF
19	Serine protease inhibitor	720	7.78E-43	+ 2.8975	+ 0.5775	MF,CC, BP
20	i-type lysozyme 2	1561	5.41E-74	+ 2.6021	− 0.0040	MF

exterior part of the lobules through the immobilized more mature cells in the inner part, where they can be released into the haemal lacunae (Fig. 4A). In contrast, MrALF mRNA is highly expressed in the precursor cells in the exterior part of the lobules (Fig. 4B). These results indicated that immune-related genes are expressed in the precursor cells to ensure that all released hemocytes are ready to resist infection, whereas cell growth-involved genes can be expressed in all cell types in the hematopoietic tissue in order to increase the mitotic division and number of hemocytes for homeostasis.

3.5. Validation of gene alternation from unigenes after MrNV infection by qRT-PCR

To validate the results from the RNA sequencing data, four unigenes including MrCHF, mitotic-spindle organizing 1-like (MSO) (Acc. No. MH883364), anti-lipopolysaccharide factor (ALF) (Acc. No. MH846235), and heat shock protein 70 (HSP70) (Acc. No. MH846234) were selected for qRT-PCR analysis. At 6 h, all genes were significantly

enhanced, having MSO and ALF to approach their highest level, whereas the expressions of CHF and HSP70 reached their maximal levels at 12 h (Fig. 5). This result well corresponded the RNAseq data, confirming that the Hpt cells simultaneously upregulate cell growth and immune-related gene enhancement at the early stage of viral infection. However, this response occurs temporally in the short term period – all of the genes studied returned to a normal level within 24 h.

4. Discussion

Principally, hemocyte proliferation takes place in specialized Hpt, where it provides an environment for either undifferentiated blood stem cells to undergo a self-renewal or offspring differentiation [18]. Therefore, comparative transcriptome analysis of directed molecular responses using next-generation sequencing and bioinformatic techniques is a powerful approach to rapidly generate large amounts of data [19] on categories such as biological processes, cellular components and molecular function in response to a pathogenic infection. Through

Table 3
Top 20 down regulated genes at 6 h post infection.

No	Protein/Gene description	Length	E-value	Fold change (log2)		Ontology (level 2)
				6 h	24 h	
1	Hypothetical protein TTRE_0000975601	380	2.97E-17	− 6.4800	− 0.5667	N/A
2	Calcified cuticle	444	4.86E-24	− 0.6569	− 3.4206	MF
3	Uncharacterized threonine-rich GPI-anchored glycoprotein	580	3.57E-25	− 0.6719	− 2.7226	N/A
4	Strongly chitin-binding −1	376	6.61E-18	− 0.7240	− 2.1418	MF
5	Cytochrome c oxidase subunit III (mitochondrion)	425	5.09E-71	− 3.4255	− 0.9587	MF,CC,BP
6	Early cuticle 6	611	3.91E-44	− 0.3154	− 2.5236	MF
7	Hypothetical cuticle	862	2.91E-34	− 0.8259	− 1.9778	MF
8	Structural constituent of cuticle	1154	3.04E-23	− 1.8823	− 0.8361	MF
9	Glycine-rich cell wall structural -like	1005	3.81E-20	− 2.0326	− 1.1506	MF,CC,BP
10	Tubulin alpha-8 chain	1252	9.85E-135	− 1.6431	− 0.3598	MF,CC,BP
11	Transmembrane 258	366	1.30E-39	− 1.8832	+ 3.4739	CC
12	C-type lectin	1214	4.57E-43	− 0.1993	− 1.9640	MF
13	Larval cuticle LCP-17-like	1163	6.26E-34	− 1.1985	− 0.9319	MF
14	Calpain T	1646	8.99E-39	− 2.3735	+ 0.5493	MF
15	Microfibril-associated glyco 4-like	1705	3.73E-144	− 0.8395	− 1.3739	N/A
16	U6 snRNA-associated Sm LSm5	619	1.19E-49	− 2.8272	+ 1.2087	MF,CC,BP
17	Juvenile hormone esterase 1	3538	4.91E-139	− 0.3825	− 1.3812	MF
18	PREDICTED: rootletin-like	5380	1.52E-20	− 1.5709	+ 0.4957	N/A
19	Reverse transcriptase	4402	2.43E-63	− 1.8402	+ 0.8376	MF, BP
20	Histone H1-delta-like	425	2.11E-34	+ 0.1338	− 1.6960	MF,CC,BP

Table 4
DEGs associated with immune system and cell growth regulation during MrNV infection.

No	Protein/Gene description	Length	E-value	Fold change (log2)		Ontology (level 2)
				6 h	24 h	
Immune-related gene						
1	C-type lectin	1214	4.57E-43	−0.1993	−1.9640	MF
2	Serine ase inhibitor	720	7.78E-43	+2.8975	+0.5775	MF,CC,BP
3	Anti-lipopolysaccharide factor	831	2.09E-62	+2.3837	+0.1415	N/A
4	Platelet-activating factor acetylhydrolase-like isoform X2	1559	9.79E-40	+2.1437	−0.3758	MF,BP
5	70 kDa heat shock protein form 1	1911	0	+2.1319	−0.9152	N/A
6	i-type lysozyme-like protein 2	1561	5.41E-74	+2.6021	−0.0040	MF
7	Crustin-like protein	706	8E-53	+3.4545	+1.6154	MF,CC,BP
8	Reverse transcriptase	4468	2.43E-63	−1.8402	+0.8376	MF, BP
9	Kazal-like serine protease inhibitor-like protein	535	1.87E-08	+2.1055	+0.1105	MF, BP
10	Heat shock 10	715	1.78E-37	+2.2657	−0.7881	MF,CC,BP
11	Glutathione peroxidase	1258	2.83E-70	+0.7140	−1.6610	MF, BP
12	Peroxinectin	1536	5E-153	+2.2923	+0.0572	MF,CC,BP
Cell growth regulation						
13	Crustacean hematopoietic factor like protein	679	4.55E-15	+1.9313	+1.2457	BP
14	Neuroparsin	788	2.35E-29	+2.2988	−0.3010	MF,CC,BP
15	Cell growth-regulating nucleolar protein-like	2096	3.05E-45	+2.1560	−0.2674	MF
16	Mitotic-spindle organizing 1-like	487	3.02E-21	+2.7511	−0.2358	CC,BP
17	Cell division cycle 5	3452	0	+1.2394	−1.0209	MF,BP
18	Cyclin G2	1875	0	−0.0804	−1.0494	BP
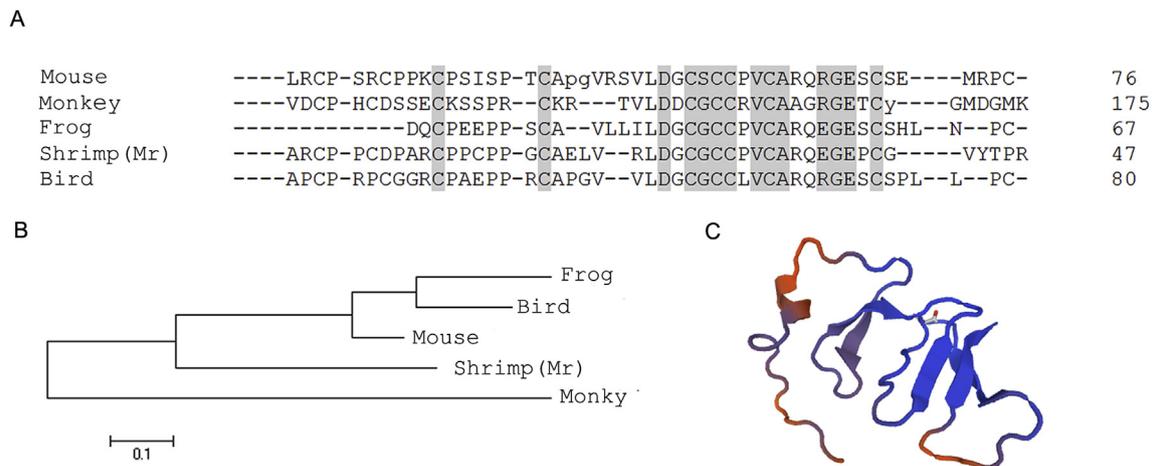
Fig. 2. Structure analysis and alignment of putative *Mr*CHF. *(A)* Multiple alignments indicating the conserved sequences *(gray)* of insulin-like growth factor-binding domain proteins *(IGFBP)* in *Mr*CHF with IGFBP from various species, phylogenetic analysis *(B)* and putative three-dimensional structure *(C)*. Mouse, *Mus musculus*, IGFBP *(*GenBank Acc No. 6754876*)*, Monkey, *Pan troglodytes*, IGFBP *(*332821365*)*, Frog, *Xenopus laevis*, IGFBP *(*147905087*)*, Bird, *Gallus gallus*, IGFBP *(*71896015*)*.
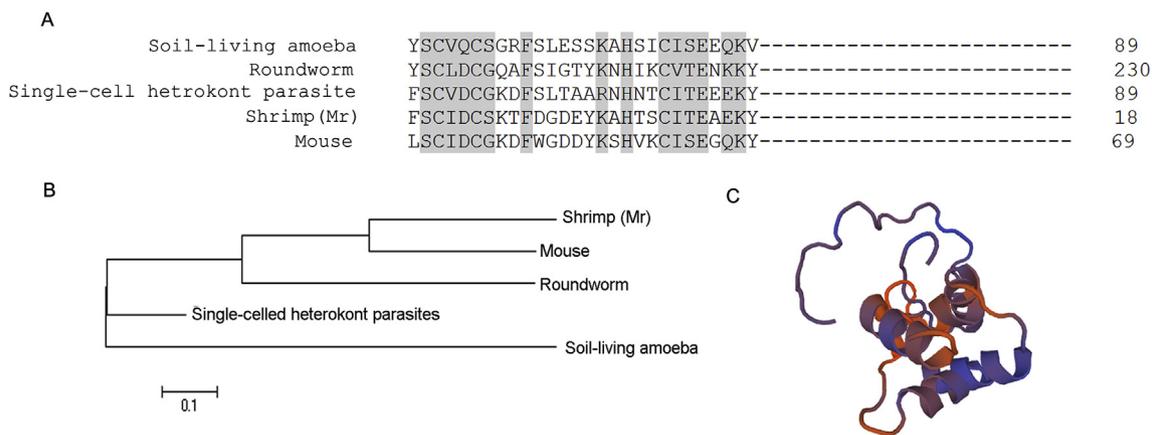
Fig. 3. Structure analysis and alignment of putative *Mr*Lyar. *(A)* Multiple alignments indicating the conserved sequences *(gray)* of the zinc finger DNA binding domain *(Lyar)* in *Mr*Lyar with Lyar from various species. Mouse, *Mus musculus*, Lyar (GenBank Acc. No.1 WJV_A), Soil-living amoeba, *Dictyostelium discoideum*, Lyar *(*74850590*)*, Single-celled heterokont parasites, *Blastocystis hominis*, Lyar *(*855316524*)*, Roundworm, *Brugia malayi*, Lyar *(*170572899*)*.
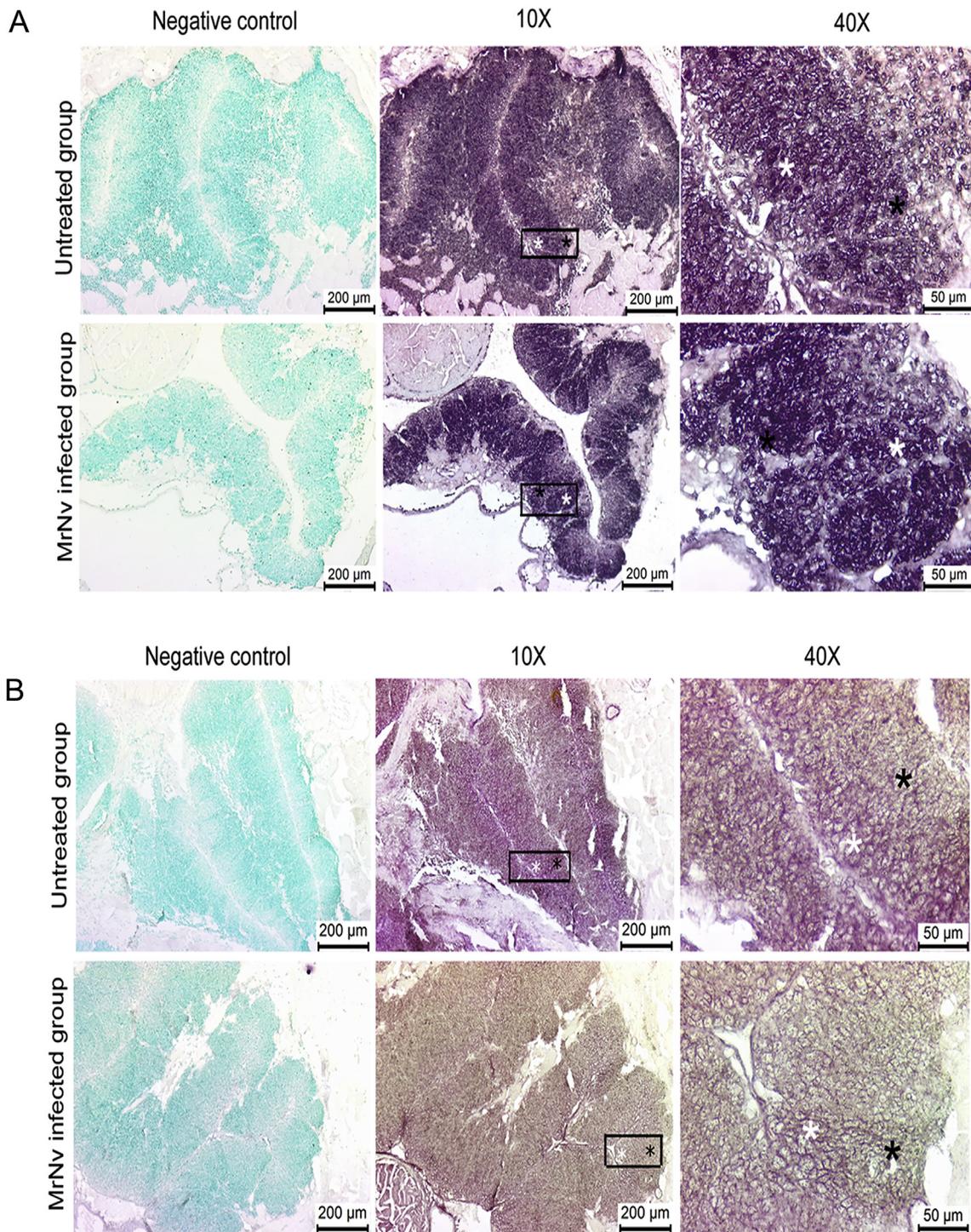
Fig. 4. *In situ* hybridization of CHF and ALF mRNAs in hematopoietic tissue cells at 0 and 6 h after MrNV infection. (A) CHF mRNA was observed in all cell types in the Hpt from the exterior (white asterisk) to the apical part (black asterisk) of the lobule. (B) ALF mRNA was predominantly observed in precursor cells at the exterior part (white asterisk) of the lobule. Bar = 200 μm and 50 μm at 10X and 40X magnification, respectively.

suppression subtractive hybridization, WSSV challenges in the red claw crayfish altered the expression of many genes in Hpt cells [20]. We thus considered using these comparative transcriptomic approaches to obtain first-hand information about gene alteration during particular viral infections, information that would be useful for antimicrobial strategic development. Here, we report on a transcriptome analysis of Hpt genes in the response to viral infection. In addition to known genes that have been documented to be involved in viral infection, genes related to the immune system of *M. rosenbergii* were newly identified in this study and

explain why adult prawn resist viral infection.

Hematopoiesis is a process by which blood stem cells differentiate and release from the Hpt into the circulation to maintain hemocyte homeostasis either in normal or harmful situations, including viral infection. In crustaceans, factors that control hematopoiesis were first documented in the crayfish *P. leniusculus* [21] and later in *L. vannamei* [22]. Sequence analysis has revealed that *Pl*CHF, *Lv*CHF and *Mr*CHF contain a conserved domain that is similar to vertebrate IGFBP, which serves as a carrier protein for insulin-like growth factor 1. A previous
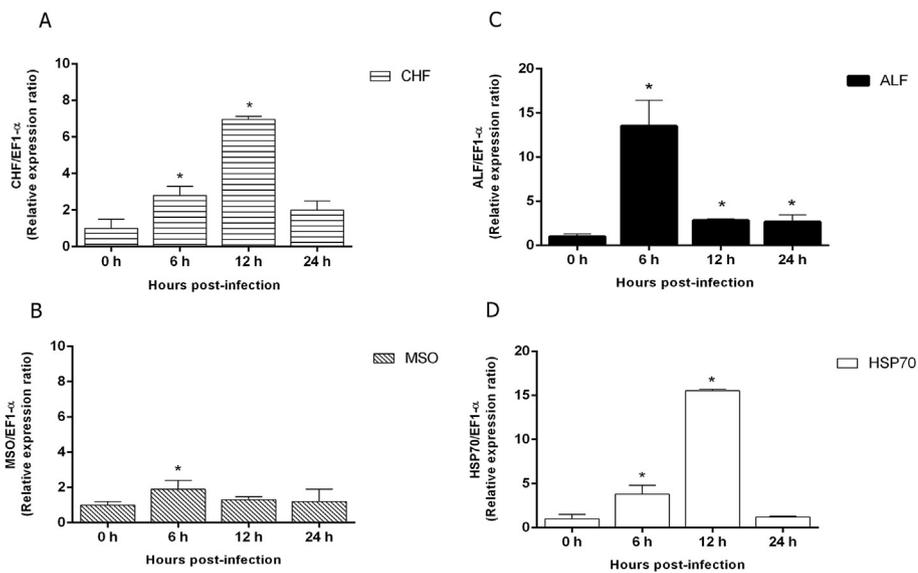
Fig. 5. The mRNA expression levels of CHF (A), MSO (B), ALF (C), and HSP70 (D) in the Hpt cells of *M. rosenbergii* at different time intervals after viral infection. The reference gene is EF1-α. Vertical bars represent the mean ± SD (N = 5). Significant differences (P < 0.05) between the viral infection and the control groups in the same exposure time are indicated with asterisks.

study demonstrated that the expression of CHF in the Hpt and semi-granular cells (SGCs) is regulated by astakine 1. CHF plays a key role as a switch that turns on different maturation lineages in hemocytes; therefore, knocking down this gene in crayfish results in a severe loss of blood cells. Our transcriptome analysis revealed that *Mr*CHF mRNA was highly expressed in the Hpt, consistent with the reports in *P. leniusculus* and *L. vannamei* [21,22]. Up-regulation of *Mr*CHF mRNA upon MrNV infection suggested that this gene was triggered during viral infection and subsequently accelerated hemocyte proliferation, differentiation and release into the circulatory system. In addition to *Mr*CHF, a protein containing the cell growth-regulating zinc finger (Lyar) domain, which plays an important role in controlling self-renewal and differentiation of embryonic stem cells (ESCs) [23], was also up-regulated in Hpt tissue. During hematopoiesis, high expression of Lyar has been reported in erythroid progenitor cells from early to mid-maturation. Knocking down Lyar severely affected the cell differentiation process, leaving only undifferentiated cells in the Hpt [24]. The conserved domain between the *Mr*Lyar protein and that of mice might imply that *Mr*Lyar plays the same role as mammalian Lyar in promoting hematopoiesis. Mitotic-spindle organizing (MSO) proteins have been reported to be associated with a ring of gamma-tubulin (γ-TuRC*)* complex which is essential for spindle assembly and chromosome segregation [25]. An up-regulation of MSO in Hpt during viral infection and environmental alterations suggests the response of Hpt to viral infection by increasing the mitotic process to produce new daughter cells for maintaining the physiological homeostasis.

The other mechanisms of viral resistance in crustaceans rely on both immune-related and nonimmune-related gene enhancement in the Hpt tissue of the infected animals [9,20]. Upon MrNV infection, 462 unigenes were differentially expressed in the infected animals as compared to the control ones. Two best examples of the immune-related genes that are extensively studied are C-type lectin (a pattern-recognition protein participated in carbohydrate binding of the pathogen) and HSP70 (a stress response protein or molecular chaperone). C-type lectin is down-regulated during early stage of MrNV infection (Table 3). In fact, suppression of this gene during early phase of virus infection has also been evident in WSSV infected *L. vannamei* and *F. chinensis* [26–28]. This piece of information suggests that down-regulation of this genes might correspond and serve as a potential marker for an early stage of the viral infection. HSP70 is involved in WSSV suppression [29] and *V. parahaemolyticus* resistance through immune activation [30]. Up-regulation of this gene at 6 h suggests the function of this gene in provoking immune system against early MrNV infection. Apart from genes participated in immune system, other nonimmune-related genes

also play important roles in other biological processes in response to viral infection. Some well-established processes include DNA unwinding or repair by topoisomerase II alpha [31–33] and provoking inflammation by serum amyloid A in vertebrate species [34]. This gene also significantly altered during MrNV infection which was among the top 20 up- and down-regulated genes (Tables 2 and 3). Interestingly, a large numbers of proteases, enzymes and some inhibitors have also been reported to be involved in innate immune response against virus and/or bacteria in crustaceans including shrimp. Kazal type protease inhibitor, SPIPm2, has been reported to interact with a WSSV viral protein 447 and inhibited WSSV replication in infected *P. monodon* [35,36]. Serine type protease inhibitor, Type III crustin and clip domain serine protease has been demonstrated to engage antimicrobial activity and prophenol oxidase activation [37–39] and were shown herein to be up-regulated during MrNV infection (Table 2). In addition, a novel invertebrate (i-type) lysozyme mRNA homolog was firstly identified and up-regulated in Hpt tissue in this study (Table 2). It is reported that i-type lysozyme possesses antimicrobial property without muramidase activity [40], and this enzyme is significantly altered in WSSV infected *M. japonicus* tissues, suggesting its viral responsive function [41]. Finally, shrimp endogenous reverse transcriptase, firstly identified in *M. japonicus,* exhibits anti-viral activity against WSSV and *V. alginolyticus* infection [42]. During MrNV infection, this gene was down-regulated at 6 h p.i. and gradually increased at 24 h p.i. suggesting its viral clearance and immune responsive actions against this viral infection.

To the best of our knowledge, there is only one study [43] that has reported the use of *in situ* hybridization to localize immune-related genes in this organ. The results revealed that prophenoloxidase (proPO) found in semigranular and granular cells is absent in the Hpt of crayfish, suggesting that proPO must be produced immediately before or after hemocyte release from the Hpt. In the present study, we demonstrated that anti-lipopolysaccharide factor (ALF), a broad-spectrum antimicrobial peptide that is also involved in the anti-WSSV response [44], was present in the Hpt, especially in the precursor stem cell population (Fig. 4). Therefore, it is feasible that the onset of production of each immune gene in the hemocyte is different (generalized immune-related genes are produced first, followed by the more complex systemic genes). In this regard, we found the positive hybridization signal of MrCHF mRNA in the Hpt, which agreed well with its RNA sequencing data. Together, it is suggested that disturbing prawn homeostasis by viral infection will trigger the expression of mRNAs related not only to cell proliferation but also to the immune system, and these immune genes are firstly synthesized in the Hpt stem cells before being released into the circulatory system.

In conclusion, transcriptome analysis of the MrNV infected Hpt in *M. rosenbergii* was performed in this study. The results showed the up-regulation of multiple genes, including cell growth regulators and immune-related genes involved in MrNV resistance. It is suggested a dual role of Hpt in defensive response and hemocytes proliferation. Further investigations of these molecules might be useful for the development of anti-MrNV therapy targets and viral management.

Acknowledgements

References

[1] I.S. Azad, M.S. Shekhar, A.R. Thirunavukkarasu, M. Poornima, M. Kailasam, J.J.S. Rajan, et al., Nodavirus infection causes mortalities in hatchery produced larvae of Lates calcarifer: first report from India, Dis. Aquat. Organ. 63 (2005) 113–118.
[2] J.R. Bonami, Z. Shi, D. Qian, J.S. Widada, White tail disease of the giant freshwater prawn, *Macrobrachium rosenbergii*: separation of the associated virions and characterization of MrNV as a new type of nodavirus, J. Fish. Dis. 28 (2005) 23–31.
[3] A.S.S. Hameed, K. Yoganandhan, J.S. Widada, J.R. Bonami, Experimental transmission and tissue tropism of *Macrobrachium rosenbergii* nodavirus (MrNV) and its associated extra small virus (XSV), Dis. Aquat. Organ. 62 (2004) 191–196.
[4] A.S. Sahul Hameed, M.X. Charles, M. Anilkumar, Tolerance of *Macrobrachium rosenbergii* to white spot syndrome virus, Aquaculture 183 (2000) 207–213.
[5] M. Sarathi, A. Nazeer Basha, M. Ravi, C. Venkatesan, B. Senthil Kumar, A.S. Sahul Hameed, Clearance of white spot syndrome virus (WSSV) and immunological changes in experimentally WSSV-injected *Macrobrachium rosenbergii*, Fish Shellfish Immunol. 25 (2008) 222–230.
[6] P.K. Sahoo, B.R. Pillai, J. Mohanty, J. Kumari, S. Mohanty, B.K. Mishra, In *vivo* humoral and cellular reactions, and fate of injected bacteria *Aeromonas hydrophila* in freshwater prawn *Macrobrachium rosenbergii*, Fish Shellfish Immunol. 23 (2007) 327–340.
[7] I. Söderhäll, E. Bangyeekhun, S. Mayo, K. Söderhäll, Hemocyte production and maturation in an invertebrate animal; proliferation and gene expression in hematopoietic stem cells of *Pacifastacus leniusculus*, Dev. Comp. Immunol. 27 (2003) 661–672.
[8] X. Lin, I. Söderhäll, Crustacean hematopoiesis and the astakine cytokines, Blood 117 (2011) 6417–6424.
[9] J. Jeswin, X.L. Xie, Q.L. Ji, K.J. Wang, H.P. Liu, Proteomic analysis by iTRAQ in red claw crayfish, *Cherax quadricarinatus*, hematopoietic tissue cells post white spot syndrome virus infection, Fish Shellfish Immunol. 50 (2016) 288–296.
[10] P. Jariyapong, A. Pudgerd, W. Weerachatyanukul, I. Hirono, S. Senapin, A.K. Dhar, et al., Construction of an infectious *Macrobrachium rosenbergii* nodavirus from cDNA clones in Sf9 cells and improved recovery of viral RNA with AZT treatment, Aquaculture 483 (2018) 111–119.
[11] A.M. Bolger, M. Lohse, B. Usadel, Trimmomatic: a flexible trimmer for Illumina sequence data, Bioinformatics 30 (2014) 2114–2120.
[12] M.G. Grabherr, B.J. Haas, M. Yassour, J.Z. Levin, D.A. Thompson, I. Amit, et al., Trinity: reconstructing a full-length transcriptome without a genome from RNA-Seq data, Nature Biotechnol. 29 (2011) 644–652.
[13] F. Kiefer, K. Arnold, M. Künzli, L. Bordoli, T. Schwede, The SWISS-MODEL Repository and associated resources, Nucleic Acids Res. 37 (2009) D387–D392.
[14] C. Chotwiwatthanakun, W. Santimanawong, P. Sobhon, S. Wongtripop, R. Vanichviriyakit, Inhibitory effect of a reproductive-related serpin on sperm trypsin-like activity implicates its role in sperm maturation of *Penaeus monodon*, Mol. Reprod. Dev. 85 (2018) 205–214.
[15] T. Christian, W. Christine, K. Urs, B. Claudia, B. Tommy, K.N. Lucia, et al., Structural and biochemical characterization of native and recombinant single insulin-like growth factor-binding domain protein (SIBD-1) from the Central American Hunting Spider *Cupiennius salei* (Ctenidae), Proteins: Struct. Funct. Bioinf. 80 (2012) 2323–2329.
[16] N. Yang, Z. Yu, M. Hu, M. Wang, R. Lehmann, R.M. Xu, Structure of *Drosophila Oskar* reveals a novel RNA binding protein, Proc. Natl. Acad. Sci. U.S.A. 112 (2015) 11541–11546.
[17] A. Gallo, C. Lo Sterzo, M. Mori, A. Di Matteo, I. Bertini, L. Banci, et al., Structure of nucleophosmin DNA-binding domain and analysis of its complex with a G-quadruplex sequence from the c-MYC Promoter, J. Biol. Chem. 287 (2012) 26539–26548.
[18] M. Grigorian, V. Hartenstein, Hematopoiesis and hematopoietic organs in arthropods, Dev. Gene. Evol. 223 (2013), https://doi.org/10.1007/s00427-012-0428-2.
[19] S. Li, X. Zhang, Z. Sun, F. Li, J. Xiang, Transcriptome analysis on Chinese shrimp *Fenneropenaeus chinensis* during WSSV acute infection, PLoS One 8 (2013) e58627.
[20] H.P. Liu, R.Y. Chen, Q.X. Zhang, H. Peng, K.J. Wang, Differential gene expression profile from haematopoietic tissue stem cells of red claw crayfish, *Cherax quadricarinatus*, in response to WSSV infection, Dev. Comp. Immunol. 35 (2011) 716–724.
[21] X. Lin, K. Söderhäll, I. Söderhäll, Invertebrate hematopoiesis: an astakine-dependent novel hematopoietic factor, J. Immunol. 186 (2011) 2073–2079.
[22] W. Charoensapsri, P. Sangsuriya, T. Lertwimol, W. Gangnonngiw, K. Phiwsaiya, S. Senapin, Laminin receptor protein is implicated in hemocyte homeostasis for the whiteleg shrimp *Penaeus (Litopenaeus) vannamei*, Dev. Comp. Immunol. 51 (2015) 39–47.
[23] L. Hui, W. Beibei, Y. Acong, L. Rui, W. Weicheng, Z. Yang, et al., Ly-1 Antibody reactive clone is an important nucleolar protein for control of self-renewal and differentiation in embryonic stem cells, Stem Cell. 27 (2009) 1244–1254.
[24] J. Ju, Y. Wang, R. Liu, Y. Zhang, Z. Xu, Y. Wang, et al., Human fetal globin gene expression is regulated by LYAR, Nucleic Acids Res. 42 (2014) 9740–9752.
[25] J.R.A. Hutchins, Y. Toyoda, B. Hegemann, I. Poser, J.K. Hériché, M.M. Sykora, et al., Systematic characterization of human protein complexes identifies chromosome segregation proteins, Science (New York, NY) 328 (2010) 593–599.
[26] Z.Y. Zhao, Z.X. Yin, X.P. Xu, S.P. Weng, X.Y. Rao, Z.X. Dai, et al., A novel C-type lectin from the shrimp *Litopenaeus vannamei* possesses anti-white spot syndrome virus activity, J. Virol. 83 (2009) 347.
[27] T.H.T. Ma, S.H.K. Tiu, J.G. He, S.M. Chan, Molecular cloning of a C-type lectin (LvLT) from the shrimp *Litopenaeus vannamei*: early gene down-regulation after WSSV infection, Fish Shellfish Immunol. 23 (2007) 430–437.
[28] Y.C. Liu, F.H. Li, B. Dong, B. Wang, W. Luan, X.J. Zhang, et al., Molecular cloning, characterization and expression analysis of a putative C-type lectin (Fclectin) gene in Chinese shrimp *Fenneropenaeus chinensis*, Mol. Immunol. 44 (2007) 598–607.
[29] Y.R. Lin, H.C. Hung, J.H. Leu, H.C. Wang, G.H. Kou, et al., The role of aldehyde dehydrogenase and Hsp70 in suppression of white spot syndrome virus replication at high temperature, J. Virol. 85 (2011) 3517–3525.
[30] W. Junprung, P. Supungul, A. Tassanakajon, Litopenaeus vannamei heat shock protein 70 (LvHSP70) enhances resistance to a strain of *Vibrio parahaemolyticus*, which can cause acute hepatopancreatic necrosis disease (AHPND), by activating shrimp immunity, Dev. Comp. Immunol. 90 (2019) 138–146.
[31] P. Luthra, S. Aguirre, B.C. Yen, C.A. Pietzsch, M.T. Sanchez-Aparicio, B. Tigabu, et al., Topoisomerase II inhibitors induce DNA damage-dependent interferon responses circumventing Ebola virus immune evasion, mBio 8 (2017) e00368-17, , https://doi.org/10.1128/mBio.00368-17.
[32] H. Imai, H. Dansako, Y. Ueda, S. Satoh, N. Kato, Daunorubicin, a topoisomerase II poison, suppresses viral production of hepatitis B virus by inducing cGAS-dependent innate immune response, Biochem. Biophys. Res. Commun. 504 (2018) 672–678.
[33] P. Bouillé, F. Subra, J.F. Mouscadet, C. Auclair, Antisense-mediated repression of DNA topoisomerase II expression leads to an impairment of HIV-1 replicative cycle, J. Mol. Biol. 285 (1999) 945–954.
[34] K.K. Eklund, K. Niemi, P.T. Kovanen, Immune functions of serum amyloid A, Crit. Rev. Immunol. 32 (2012) 335–348.
[35] S. Donpudsa, S. Ponprateep, A. Prapavorarat, S. Visetnan, A. Tassanakajon, V. Rimphanitchayakit, A Kazal-type serine proteinase inhibitor SPIPm2 from the black tiger shrimp *Penaeus monodon* is involved in antiviral responses, Dev. Comp. Immunol. 34 (2010) 1101–1108.
[36] S. Ponprateep, K. Phiwsaiya, A. Tassanakajon, V. Rimphanitchayakit, Interaction between Kazal serine proteinase inhibitor SPIPm2 and viral protein WSV477 reduces the replication of white spot syndrome virus, Fish Shellfish Immunol. 35 (2013) 957–964.
[37] Y. Liu, T. Liu, F. Hou, X. Wang, X. Liu, Lvserpin3 is involved in shrimp innate immunity via the inhibition of bacterial proteases and proteases involved in prophenoloxidase system, Fish Shellfish Immunol. 48 (2016) 128–135.
[38] S. Visetnan, P. Supungul, A. Tassanakajon, S. Donpudsa, V. Rimphanitchayakit, A single WAP domain-containing protein from *Litopenaeus vannamei* possesses anti-proteinase activity against subtilisin and antimicrobial activity against AHPND-inducing *Vibrio parahaemolyticus*, Fish Shellfish Immunol. 68 (2017) 341–348.
[39] N. Khorattanakulchai, P. Amparyup, A. Tassanakajon, Binding of PmClipSP2 to microbial cell wall components and activation of the proPO-activating system in the black tiger shrimp *Penaeus monodon*, Dev. Comp. Immunol. 77 (2017) 38–45.
[40] P. Supungul, V. Rimphanitchayakit, T. Aoki, I. Hirono, A. Tassanakajon, Molecular characterization and expression analysis of a c-type and two novel muramidase-deficient i-type lysozymes from *Penaeus monodon*, Fish Shellfish Immunol. 28 (2010) 490–498.
[41] H.T. Liu, J. Wang, Y. Mao, M. Liu, S.F. Niu, Y. Qiao, et al., Identification and expression analysis of a new invertebrate lysozyme in Kuruma shrimp (*Marsupenaeus japonicus*), Fish Shellfish Immunol. 49 (2016) 336–343.
[42] X. Ma, B. Sun, F. Zhu, Molecular cloning of Kuruma shrimp *Marsupenaeus japonicus* endonuclease-reverse transcriptase and its positive role in white spot syndrome virus and *Vibrio alginolyticus* infection, Fish Shellfish Immunol. 73 (2018) 297–308.
[43] M.W. Johansson, P. Keyser, K. Sritunyalucksana, Söderhäll Crustacean haemocytes and haematopoiesis, Aquaculture 191 (2000) 45–52.
[44] H. Liu, P. Jiravanichpaisal, I. Söderhäll, L. Cerenius, K. Söderhäll, Antilipopolysaccharide factor interferes with white spot syndrome virus replication in *vitro* and *in vivo* in the Crayfish *Pacifastacus leniusculus*, J. Virol. 80 (2006) 10365–10371.